Evaluating the Effects of 309 and 2594 Filler Alloys on the Tensile Strength, Toughness, and Corrosion Resistance of Dissimilar Welds between Duplex S32550 and TP304 Using Multi-Process TIG and MMAW

Syukran
Department of Metallurgical and Material Engineering, Faculty of Engineering, Universitas Indonesia, Depok, Indonesia
syukran@ui.ac.id

Winarto Winarto
Department of Metallurgical and Material Engineering, Faculty of Engineering, Universitas Indonesia, Depok, Indonesia
winarto.msc@ui.ac.id (corresponding author)

Muhammad Anis
Department of Metallurgical and Material Engineering, Faculty of Engineering, Universitas Indonesia, Depok, Indonesia
anis@metal.ui.ac.id

Received: 14 February 2026 | Revised: 18 March 2026 | Accepted: 26 March 2026

 DOI: https://doi.org/10.48084/etasr.18167

ABSTRACT

This study evaluates the influence of filler alloys ER309 and ER2594 on the tensile strength, impact toughness, and corrosion resistance of dissimilar welds between duplex S32550 and austenitic TP304, produced using a combined TIG and MMAW welding process. The results demonstrate that filler 2594 outperforms filler 309 across all evaluated properties. Welded joints fabricated with filler 2594 achieved a higher Ultimate Tensile Strength (UTS) of 537.48 MPa (72.8% joint efficiency), compared to 508 MPa (68.8% efficiency) for filler 309. Charpy impact testing at –40°C further demonstrated superior toughness for filler 2594 (56.47 J) compared to filler 309 (52.73 J), which is attributed to a more favorable ferrite–austenite phase balance and higher nitrogen content. Fracture during tensile testing consistently occurred in the Heat-Affected Zone (HAZ) of the TP304 base metal, identifying this region as the primary mechanical weakness of the joint. Corrosion performance, evaluated through potentiodynamic polarization in a 1% H_2SO_4 solution, revealed a significantly lower corrosion rate for Filler 2594 (1.21 mm/a) compared to filler 309 (19.24 mm/a), representing more than an order of magnitude improvement. This enhanced resistance is associated with the higher Pitting Resistance Equivalent Number (PREN) and improved passive film stability of filler 2594. Overall, the findings indicate that filler 2594 is the optimal choice for dissimilar welding of S32550 and TP304, providing superior tensile efficiency, improved low-temperature toughness, and excellent resistance to aggressive corrosive environments.

Keywords-dissimilar welding; duplex S32550; TP304; filler 2594; filler 309; corrosion resistance; mechanical properties

I. INTRODUCTION

As the demand for durable and cost-effective structures in the petrochemical, oil and gas, and marine industries increases, optimizing welding techniques for dissimilar materials has become important. Components such as subsea manifolds, heat exchangers, piping systems, and chemical reactors must operate under high pressures and resist chloride-induced corrosion while maintaining economic efficiency. The combination of duplex and austenitic stainless steels is

particularly attractive, as it offers a balance of high mechanical strength and enhanced corrosion resistance compared to single-material systems [1, 2]. Duplex stainless steels, such as S32550, are widely used in subsea applications due to their excellent toughness and resistance to stress-corrosion cracking [3]. In contrast, austenitic stainless steels, like TP304, are preferred for high-temperature environments requiring stable and reliable performance [4]. Welding is the primary method for joining dissimilar metals, with Gas Tungsten Arc Welding (GTAW/TIG) and Shielded Metal Arc Welding (SMAW/MMAW) being among the most employed processes [5, 6]. Other techniques, including Plasma Arc Welding (PAW) [7], Laser Beam Welding (LBW) [8], and Flux-Cored Arc Welding (FCAW) [9], are utilized in more specialized applications. The choice of the welding process plays a crucial role in determining the resulting microstructure, mechanical properties, and corrosion resistance of the joint, making it a key factor in design and fabrication [10]. Advancements, such as Hot-Wire TIG and the application of Post-Weld Heat Treatment (PWHT), reduce residual stresses and improve mechanical performance [11]. Nevertheless, MMAW is widely employed in industrial and field applications due to its versatility and cost-effectiveness, particularly in the welding of nickel-based superalloys, such as Inconel 718, to austenitic stainless steels [12].

Despite the practical prevalence of combining TIG and MMAW for repair and fabrication, detailed studies on the metallurgical interactions and structural performance of this multi-process approach are limited, particularly for the Duplex S32550 and TP304 pairing. Dissimilar welding introduces complex phenomena: interdiffusion of Fe, Cr, and Ni across the fusion boundary, macrosegregation, formation of secondary interdendritic phases (e.g., Nb-rich Laves or Mo-rich carbides), and accumulation of residual stresses from multi-pass welding [13, 14]. These features can produce local hardness increases, reduced toughness, increased susceptibility to corrosion, and distortion, necessitating careful control of welding parameters and filler selection [14, 15]. Mitigation strategies to address these challenges include the use of Ni-based buttering layers to reduce chemical gradients, as well as optimized groove designs (e.g., double V-grooves) to minimize distortion and residual stresses [13, 16]. Among the various factors influencing joint performance, filler metal composition plays a significant role. The effectiveness of different filler materials has been evaluated. Authors in [17] compared ERNiCrMo-4, ERNiCrMo-3, and ER309L for welding UNS S32750 to AISI 304 and reported that ERNiCrMo-4 provided the highest impact toughness. Authors in [18] investigated ER2594, ER312, and ER385 for dissimilar welding of duplex S32205 and 316L stainless steel, concluding that ER385 exhibited superior pitting corrosion resistance. Authors in [19] examined ER2594 and ERNiCrMo-3 for joining duplex 2507 to Inconel 625 and found that both fillers delivered excellent pitting corrosion resistance in simulated marine environments, along with satisfactory tensile properties. Authors in [20] evaluated ER-NiCr-3, ER-NiCrMo-3, and ER-NiCrCoMo-1 for dissimilar welding of SA335 Gr. P11 and Incoloy 800, demonstrating that ER-NiCrMo-3 achieved the best combination of tensile strength and impact toughness. However, most prior work on duplex–austenitic dissimilar welding has focused on single welding processes and commonly studied duplex grades other than duplex S32550, leaving relatively little experimental data for the duplex S32550 and TP304 combination. Moreover, the combined use of TIG and MMAW, which is frequently employed in industrial practice, is under-investigated for this material pair. The present study addresses these gaps by evaluating the effects of two filler alloys (309 and 2594), applied with a combined TIG and MMAW procedure, on the tensile strength, impact toughness, and corrosion resistance of dissimilar duplex S32550 and TP304 welds. The objective is to provide practical guidance on filler selection and welding-parameter optimization for demanding industrial environments where single-process data are insufficient.

II. MATERIAL AND METHODOLOGY

In this study, the base pipes used were duplex S32550 and austenitic stainless steel TP304, 4-inch-diameter, schedule 40 pipes. Filler metals used during welding were alloys 2594 and 309. Before welding, samples from the base materials were analyzed using a Bruker Optical Emission Spectroscopy (OES), and the results yielded the chemical compositions of the base materials, duplex S32550 and TP304. The chemical compositions of the filler alloys were obtained from the manufacturer's data sheet [21]. Table I outlines the results of OES tests for base metals and filler alloys.

TABLE I. CHEMICAL COMPOSITION OF MATERIAL AND FILLER METAL

Materials	**Chemical composition (%wt.)**					
	Duplex S32550	TP 304	ER 309	E309-16	ER 2594	E2594-16
C	0.01	0.04	0.05	0.07	0.01	0.03
Mn	0.85	1.32	1.6	1.0	0.6	0.7
Si	0.42	0.65	0.47	0.40	0.4	0.55
Cr	24.2	18.2	23.1	23.9	24.8	25.4
Ni	5.55	9.48	13.6	13.4	9.2	9.3
Mo	3.24	0.2	0.10	0.21	3.8	3.9
Cu	0.39	0.13	0.12	0.12	0.1	0.05
Fe	64.9	69.5	Bal.	Bal.	Bal.	Bal.
N	0.15	0.08	-	-	0.26	0.24
Al	0.01	0.08				
Co	0.12	0.06				
Ti	0.01	0.01				
Nb	0.06	0				
UTS, min (Mpa)	760	515	580	590	859	935
PREN	37.3	20.1	23.4	24.6	41.5	42.1

The joint design used in this study featured a single V-groove with a 65° included angle, a 2.5 mm root opening, and a 2 mm root face, as shown in Figure 1. A hybrid welding method was employed, combining Tungsten Inert Gas (TIG) and Manual Metal Arc Welding (MMAW). TIG welding with Direct Current Electrode Negative (DCEN) was used for the root pass (1) and hot pass (2), while MMAW with Direct Current Electrode Positive (DCEP) was applied for the filler pass (3) and capping pass (4). All welding was performed using a Migatronic PI250/350A machine, following the parameters exhibited in Table II. To ensure weld integrity and prevent oxidation, shielding and purging were done using Ultra-High

Purity (UHP) and High Purity (HP) argon at a flow rate of 10–15 L/min [22]. For the TIG process, a 2.4 mm diameter 2% lanthanated tungsten electrode was used. To reduce the effects of high thermal gradients during welding, a preheating temperature of 150°C was applied [23]. Heat input was managed by adjusting the travel speed and maintaining a consistent interpass temperature, monitored with a calibrated laser pyrometer. The interpass temperature was kept below 230°C to minimize excessive thermal cycling in the HAZ and prevent slow cooling rates that could harm corrosion resistance and toughness [23]. All key process parameters for TIG and MMAW were logged in real-time by a PLX-DAQ R2.0 data logger, enabling precise monitoring of the thermal cycle.

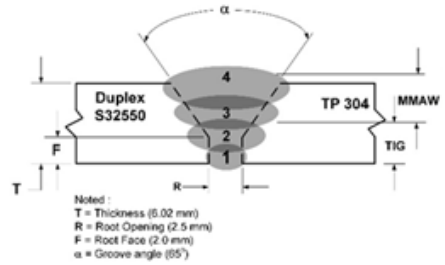

(a)

(b)

(c)

Fig. 1. Dissimilar welding processes for Duplex S32550 and TP304: (a) joint design and welding sequence, (b) TIG-MMAW welding process, (c) results of welded joints with filler 309 (J1A) and 2594 (J2A).

TABLE II. WELDING PARAMETERS

Welding process	TIG	MMAW
Polarity	DCEN	DCEP
Filler metal (TIG)	ER309	E309-16
Filler metal (MMAW)	ER2594	E2594-16
Filler diameter (mm)	2.4	2.6
Current (A)	115 - 165	70 – 80
Voltage (V)	11-13	22 – 25
Travel speed (mm/min)	40 - 90	80 - 110

To evaluate the integrity and quality of the welded joints, a comprehensive post-welding assessment was conducted. Initial inspection involved non-destructive radiographic testing in accordance with [24], employing an Iridium-192 gamma-ray source to ensure that the specimens were free from internal defects, such as porosity or inclusions. The radiographic results confirmed the sound quality and internal soundness of the welds. Furthermore, high-quality macrographs were obtained to provide a detailed visualization of the weld bead profiles, as presented in Figure 2. The cross-sectional analysis distinguishes the transition between the TIG root/hot passes (layers 1–2) and the MMAW filler/capping passes (layers 3–4) for both alloys (309 and 2594), as further detailed in Figure 3. This macrostructural evaluation confirms full penetration, excellent inter-run fusion, and a well-defined fusion zone between the TP304 and duplex S32550 base metals.

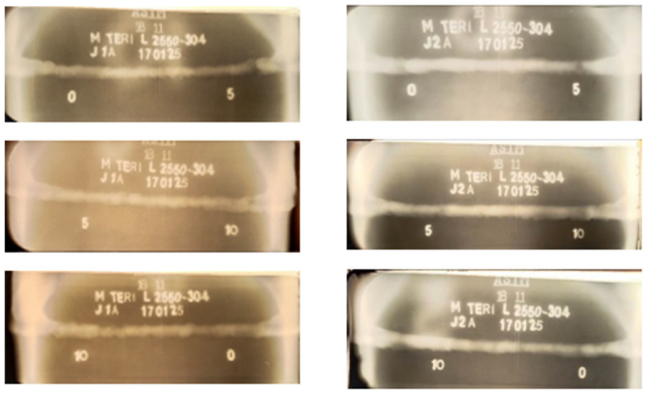

(a) (b)

Fig. 2. Radiographic image of the duplex S32550-TP304 weld joint test results: (a) joint J1A (filler-309), (b) joint J2A (filler-2594).

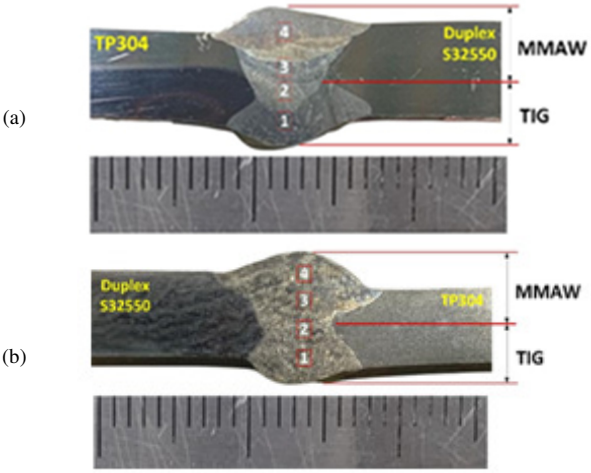

Fig. 3. High-quality macrographs showing the weld bead profiles and full penetration of the joints using: (a) Filler 309, and (b) filler 2594. Numbers 1–4 indicate the specific welding sequences for root, hot, filler, and capping passes.

Mechanical characterization included tensile testing, Vickers hardness measurements, and Charpy V-notch impact testing at −40°C. In addition, potentiodynamic polarization tests were conducted to evaluate the corrosion resistance of the welded joints. Tensile tests were carried out using a Galdabini (Italy, 2007) universal testing machine with a capacity of 100 kN. The tensile specimens were prepared in accordance with [24]. Charpy V-notch impact tests were performed at −40°C to assess the toughness of the dissimilar welded joints between duplex TP304 and S32550. The specimens were prepared

following [25]. Test locations included the TP304 base metal (BM-304), HAZ of TP304 (HAZ-304), weld metal (WM), HAZ of S32550 (HAZ-S32550), and S32550 base metal (BM-S32550). Each location was tested using three replicate specimens to ensure reliability. Before testing, the specimens were conditioned at −40°C in an ethanol-based cooling bath. The V-notch geometry was introduced using a hand broaching machine. Subsequently, corrosion behavior was evaluated using potentiodynamic polarization testing to determine key parameters, including corrosion potential (E_{corr}) and corrosion current density (I_{corr}), which are essential for assessing corrosion resistance. The electrochemical measurements were performed using a potentiostat system from CorrTest Instruments. Prior to testing, samples were sectioned to dimensions of 9 mm × 5 mm × 5 mm. For each weld, three regions were examined: base metal, HAZ, and weld metal. The measurements were conducted after immersing the samples in a 1% H_2SO_4 solution at room temperature, with a scan rate of 0.5 mV/s. A carbon electrode was used as the counter electrode, a silver/silver chloride (Ag/AgCl) electrode as the reference, and the specimen itself served as the working electrode.

III. RESULTS AND DISCUSSION

The initial evaluation of the dissimilar joints between duplex S32550 and TP304 was conducted through analysis of the stress–strain curves shown in Figure 4. Significant differences in ductility were observed between the base metals and the welded joints. In particular, the TP304 base metal exhibited substantially higher elongation before fracture compared to the welded specimens (Figure 4(a–c)), indicating that the welding process reduces the material's plastic deformation capability. The tensile test results are summarized in Table III and Figure 5. The data show that joints welded with filler 2594 achieved an average UTS of 537 MPa, compared to 508 MPa for filler 309. Although filler 2594 improves joint strength and approaches the strength of the TP304 base metal (546 MPa), both fillers produce joints with lower strength than the parent materials. Duplex S32550 exhibits a significantly higher average UTS of 738 MPa. Accordingly, the joint efficiency relative to S32550 is 72.8% for filler 2594 and 68.8% for filler 309. These results highlight the significant influence of filler metal selection on approaching the strength of the base materials. Analysis of fracture locations provides further insights into joint performance. As shown in Table III and Figure 6, all specimens consistently failed in the HAZ on the TP304 side. This fracture behavior is attributed to microstructural degradation caused by welding thermal cycles in this region. Authors in [26] reported that microstructural inhomogeneity is common in as-welded dissimilar joints, leading to a "weakest link" effect, where the most degraded region, the TP304 HAZ, governs the overall mechanical performance of the joint.

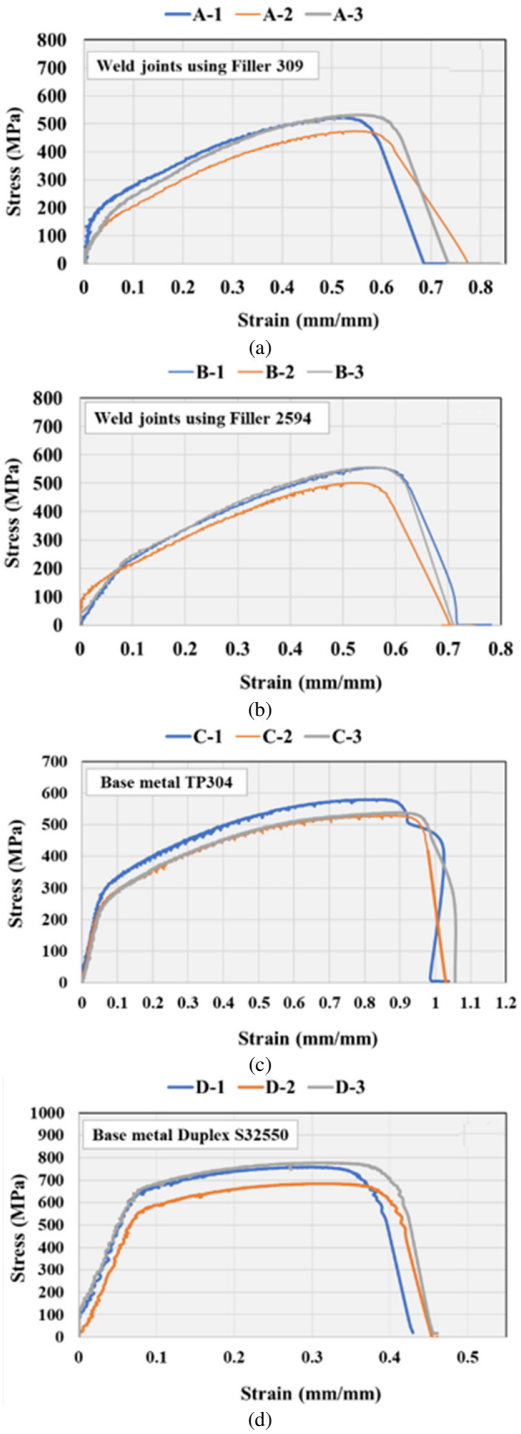

Fig. 4. Stress-strain curves for: (a) weld joints using Filler 309, (b) weld joints using Filler 2594, (c) base metal TP304, and (d) base metal Duplex S32550.

TABLE III. UTS AND JOINT EFFICIENCY OF WELD SAMPLES AND BASE METALS

Sample	UTS (Mpa)	Average UTS (Mpa)	Joint efficiency (%)	Type of failure and location
Weld joint using filler 309				
A-1	520	508	68.8%	Fracture near the HAZ of the TP304.
A-2	474			
A-3	531			
Weld joint using filler 2594				
B-1	554	537	72.8%	Fracture near the HAZ of the TP304.
B-2	501			
B-3	556			
Base metal TP304				
C-1	577	546	-	-
C-3	527			-
C-2	535			-
Base metal S32550				
D-1	756	738	-	-
D-2	683			-
D-3	774			-

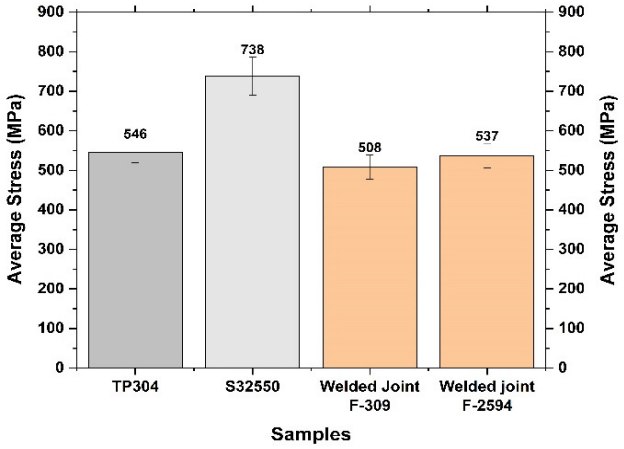

Fig. 5. Tensile test results for base metals and dissimilar welded joints between duplex S32550 and TP304.

These results differ from previous studies on dissimilar welding of super duplex 2507 and API X70 steel, where filler 309L was reported to outperform filler 2594 [27]. This discrepancy can likely be attributed to differences in base metal chemistry and variations in welding heat input. In addition, the absence of PWHT in the present study may have contributed to the observed behavior. Without PWHT, residual gradients in hardness and microstructure remain within the joint, particularly in the HAZ, leading to localized weakening [26]. These findings indicate that, although advanced fillers such as 2594 can enhance joint efficiency, effective control of thermal conditions during welding is crucial. Proper thermal management is necessary to minimize microstructural degradation in the HAZ and to maintain the overall structural integrity of dissimilar metal joints.

The results of the Charpy impact test are presented in Figure 7. It is indicated that the absorbed energy and impact energy for samples of fillers 309 and 2594 decreased significantly from the base metal to the HAZ and further into the weld metal, exhibiting a similar downward trend. This suggests that welding can adversely affect the impact energy and absorbed energy values in the material. Furthermore, for the HAZ side of 304, the impact energy value of HAZ-TP304 using filler 309 (90.15 J) is higher than that of HAZ-TP304 using filler 2594 (85.56 J). Likewise, the energy absorbed by HAZ-TP304 with filler 309 (2253.9 kJ/m²) was higher than that of filler 2594 (2139.01 kJ/m²). On the other hand, on the HAZ side of the 2550, the impact energy value of HAZ-S32550 with filler 309 (88.3 J) was lower than that of filler 2594 (100.1 J). The same applies to absorbed energy; HAZ-S32550 with filler 309 (2208.04 kJ/m²) was lower than that of filler 2594 (2502.65 kJ/m²). Figure 7 also shows that the impact energy value of TP304 base metal is slightly higher than that of duplex S32550 base metal, with an average value of 103.94 J for BM TP304 and 101.4 J for BM S32550. Similarly, the energy absorbed by TP304 base metal is also slightly higher than that of duplex S32550 base metal, with an average value of 2598.51 kJ/m² for BM TP304 and 2535.17 kJ/m² for BM S32550. For the weld metal, the impact energy value of the weld joint using filler 309 (52.73 J) was also lower than that of filler 2594 (56.47 J). Similarly, the energy absorbed in the weld joint with filler 309 (1318.39 kJ/m²) is lower than that using filler 2594 (1411.73 kJ/m²). These data indicate that the impact energy and energy absorbed during dissimilar welding between duplex S32550 and TP304 do not show too big differences between the use of filler 309 and filler 2594.

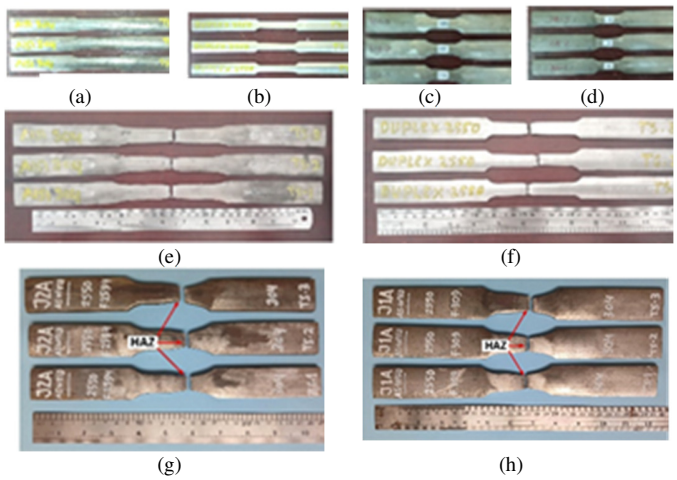

Fig. 6. Base metal and weld joint of duplex S32550 and TP304 tensile test samples: (a) base metal TP304, (b) base duplex 2550, (c) weld joint with filler 2594, (d) weld joint with filler 309, (e) base TP304 after tensile test, (f) base duplex S32550 after tensile test, (g) weld joint with filler 2594 after tensile test, (h) weld joint with filler 309 after tensile test.

The impact toughness results obtained in this study show a deviation from previous findings reported for single-pass GTAW processes, where the impact energy of dissimilar joints between duplex 2507 and API X70 exceeded 80 J. Filler 309L outperformed filler 2594, achieving weld zone impact energies of 162 J and 145 J, respectively [27]. Similarly, earlier work demonstrated that filler 309L provides higher impact strength than filler 2209 in dissimilar welds of duplex 2205 and 304L stainless steels [28]. Despite these differences, the performance of the current joints should be evaluated against established safety criteria. According to [29], the minimum acceptable impact energies at −40°C are 54 J for full-size specimens and 34 J for the HAZ and weld metal. Achieving these thresholds is

often challenging due to the formation of brittle intermetallic phases within the temperature range of 320°C-955°C during thermal cycling [29]. In the present study, however, both filler 309 and filler 2594 exceeded these requirements, indicating their suitability for industrial applications in harsh environments and their ability to maintain structural integrity despite welding-induced microstructural changes. The variation in toughness across different regions of the welded joints is primarily attributed to solidification microstructure and subsequent thermal cycles in the HAZ. In the weld metal, filler 2594 demonstrated slightly higher impact energy (56.47 J) compared to filler 309 (52.73 J), which can be attributed to a more favorable ferrite–austenite phase balance. As a super duplex alloy, filler 2594 contains higher levels of nickel and nitrogen, which promote austenite stabilization and improve resistance to crack propagation. Nevertheless, the reduction in toughness observed in the weld metal relative to the base metals (TP304 and S32550) suggests the presence of ferrite-rich microstructures or secondary phase precipitates. In the HAZ of S32550, filler 2594 also showed superior performance (100.1 J) compared to filler 309 (88.3 J). This improvement is likely due to enhanced epitaxial growth and reduced chromium nitride precipitation, which is commonly associated with high heat input in duplex stainless steels. Furthermore, macrofractographic observations (Figure 7(b)) reveal mainly ductile fracture features with lateral expansion, while localized reductions in absorbed energy indicate microstructural heterogeneity within specific regions of the joint.

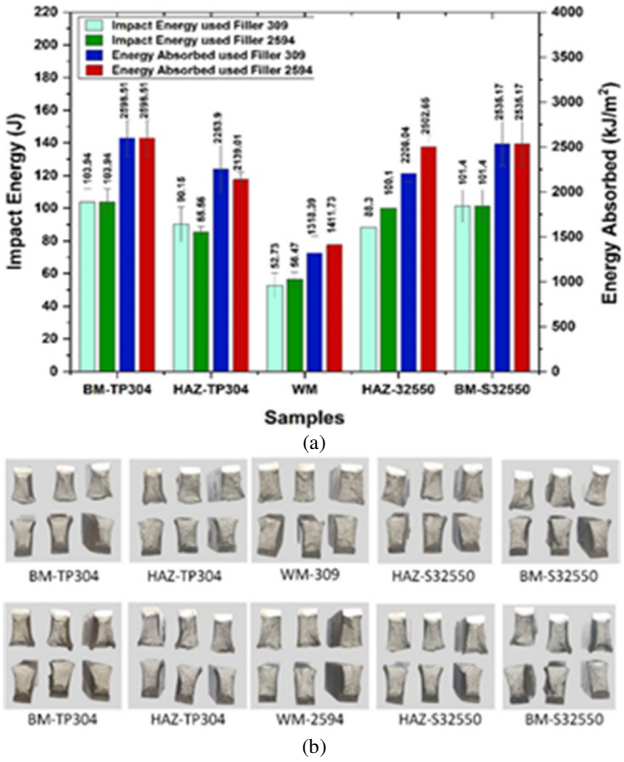

Fig. 7. Impact test results of dissimilar welding between duplex S32550 and TP304: (a) comparison of impact energy and energy absorbed for different weld zones using filler 309 and filler 2594, (b) macro-photographs of the fractured specimens after impact testing.

In subsequent stages of this research, SEM-EDX and XRD analyses will be conducted to establish a more comprehensive metallurgical correlation, enabling quantitative determination of phase fractions and identification of intermetallic precipitates such as sigma (σ) and chi (χ) phases. At present, the findings are limited to qualitative comparisons with established models and microstructural interpretations reported in [27]. The superior toughness of filler 2594 can be attributed to its solidification behavior. Filler 309 typically forms a skeletal ferrite microstructure, which may provide relatively continuous paths that facilitate crack propagation. In contrast, filler 2594 undergoes primary ferritic solidification followed by extensive transformation to reformed austenite, including Widmanstätten Austenite (WA) and Intragranular Austenite (IGA). This refined and more homogeneous microstructure contributes to improved resistance to crack initiation and propagation. Thermal control also played a critical role in the observed performance. By maintaining the interpass temperature of the S32550 HAZ below 230°C, an appropriate cooling rate was achieved, minimizing excessive ferritization and suppressing the formation of deleterious secondary phases [30]. Furthermore, the higher nickel and nitrogen contents in filler 2594 acted as strong austenite stabilizers, promoting austenite reformation during rapid thermal cycling associated with the multi-process TIG-MMAW welding technique. The combined results of impact toughness and corrosion resistance, both exceeding the acceptance criteria specified in [30], provide strong qualitative evidence of a stable and well-balanced ferrite–austenite microstructure. Although no direct quantitative phase analysis was performed, the results indicate good structural integrity and suggest the absence of harmful secondary phase precipitation within the joint. Corrosion performance was further evaluated using potentiodynamic polarization testing. The analysis focused on both weld metal and base metal regions of the dissimilar S32550–TP304 joints produced with filler 309 and filler 2594. In addition, immersion testing was conducted on weld samples fabricated with both fillers. The corresponding polarization results are presented in Figure 8 and Table IV.

TABLE IV. TAFEL ANALYSIS PARAMETER DERIVED FROM THE TAFEL MEASUREMENT

Materials	E_{corr} (*m*V)	I_{corr} (μA/cm²)	Ba (mV)	Bc (mV)	Corrosion rate (mm/a)
BMS32550	-275.33	215.15	8296.4	205.57	2.52
BM TP304	-371.42	420	4408.2	155.66	4.92
WM(F309)	-83.045	1640.2	19436	49272	19.24
WM(F2594)	38.875	103.33	160.54	996.04	1.21

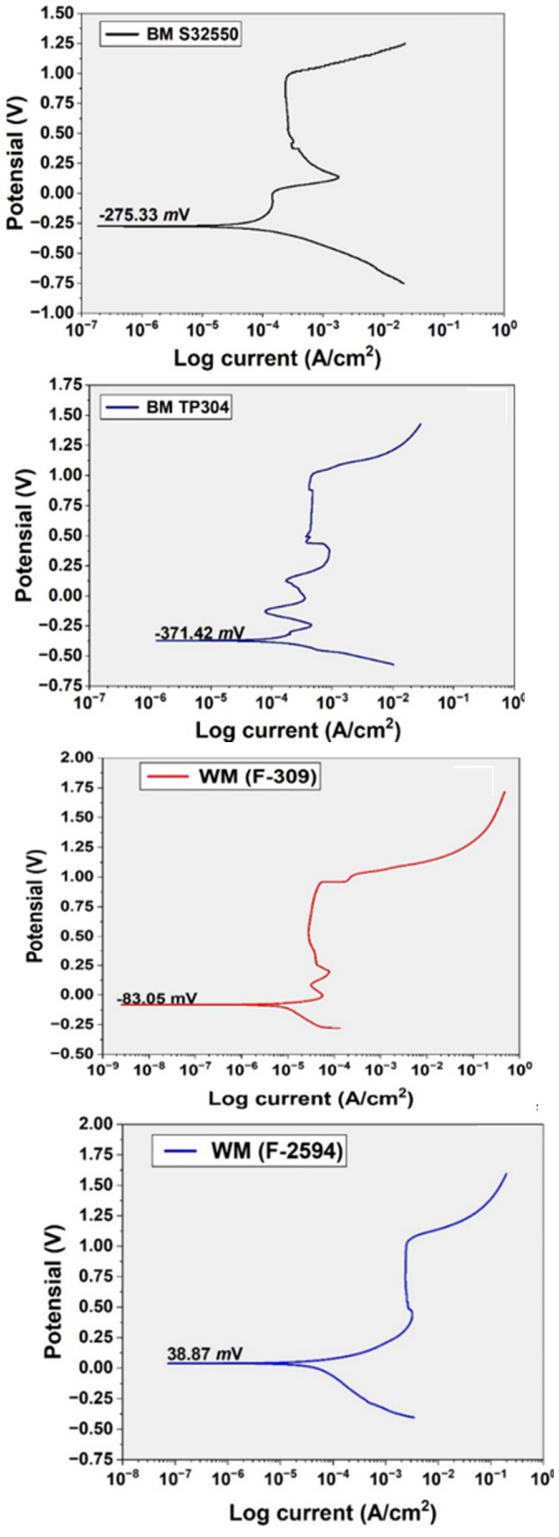

Fig. 8. Potentiodynamic polarization curves for (a) base metal S32550, (b) base metal TP304, (c) weld metal with Filler 309, and (d) weld metal with Filler 2594.

In contrast, the weld metal produced using filler 2594 exhibited the most positive corrosion potential (E_{corr} = 38.87 mV), the lowest corrosion current density (I_{corr} = 10.33 µA/cm²), and consequently the lowest corrosion rate (1.21 mm/a) among all samples. These results indicate the superior corrosion resistance of filler 2594 compared to filler 309. This trend is consistent with previous studies, which reported that in dissimilar welds of duplex 2205 and AISI 430, Filler E2209 (Epit = 0.79 V) demonstrated significantly higher pitting resistance than filler E309LMo (Epit = 0.32 V) [31]. The enhanced corrosion performance of the filler 2594 weld metal is attributed to its higher PREN and improved passive film stability. Based on its chemical composition, filler 2594 exhibits a significantly higher PREN (≈40) compared to filler 309 (≈24), due to increased concentrations of chromium (Cr), molybdenum (Mo), and nitrogen (N). These alloying elements act synergistically to promote the formation of a dense, stable, and adherent passive film, primarily composed of Cr_2O_3 and MoO_2, which effectively protects the material against chloride-induced corrosion. In contrast, the higher corrosion rate observed in the filler 309 weld metal (19.24 mm/a) is likely associated with micro-galvanic interactions between austenite and skeletal ferrite phases. The relatively low nitrogen and molybdenum content in filler 309 reduces the stability and passivation capability of the passive film once it is locally damaged. Furthermore, as supported by microstructural models in [28], the higher nitrogen content in filler 2594 not only enhances PREN but also promotes the formation of reformed austenite, leading to a more homogeneous distribution of alloying elements. This homogeneity minimizes chromium-depleted regions, suppresses pit initiation, and results in a more noble E_{corr} value compared to filler 309.

IV. CONCLUSIONS

This study systematically evaluated the effects of different filler alloys on the integrity of multi-process TIG–MMAW dissimilar joints between duplex S32550 and TP304. The results demonstrate that filler 2594 provides superior overall performance compared to filler 309. In terms of mechanical properties, filler 2594 achieved a higher UTS of 537.48 MPa, corresponding to a joint efficiency of 72.8%, whereas filler 309 reached 508 MPa (68.8% efficiency). In all cases, fracture occurred in the HAZ of TP304, identifying this region as the primary limitation in joint strength due to welding-induced thermal effects. Low-temperature impact testing at −40°C further confirmed the advantage of filler 2594, which exhibited a higher impact energy (56.47 J) compared to filler 309 (52.73 J). Both fillers exceeded the minimum safety requirements specified in [29], indicating their suitability for structural applications under subzero conditions. Corrosion performance, evaluated through potentiodynamic polarization, revealed a substantial improvement for filler 2594, which exhibited a significantly lower corrosion rate (1.21 mm/a) compared to filler 309 (19.24 mm/a), representing an improvement of more than one order of magnitude. This enhanced corrosion resistance is attributed to the higher PREN and the superior stability of the passive film associated with the 2594 alloy. Furthermore, thermal control during welding was effectively maintained using a calibrated laser pyrometer, limiting the interpass temperature to 230°C, while real-time monitoring

with a PLX-DAQ R2.0 data logger ensured consistent heat input and an optimal cooling rate. These controlled conditions, combined with the elevated nickel and nitrogen content of filler 2594, contributed to a stable ferrite–austenite phase balance, even in the absence of direct quantitative phase analysis. Overall, the findings indicate that filler 2594 is the preferred choice for dissimilar welding of S32550 and TP304, owing to its favorable chemical composition and compatibility with controlled thermal management, resulting in improved tensile performance, enhanced toughness at subzero temperatures, and superior resistance to aggressive corrosive environments.

DECLARATION OF COMPETING INTERESTS

The authors declare that they have no competing interests.

ACKNOWLEDGMENT

The authors gratefully acknowledge the financial support provided by the Indonesian Education Scholarship, the Center for Higher Education Funding and Assessment, and the Indonesian Endowment Fund for Education. Their sponsorship made the research and publication of this article possible.

DATA AVAILABILITY

The data supporting the findings of this study are available from the corresponding author upon reasonable request.

AI USE AND DECLARATION OF GENERATIVE AI USE

During the preparation of this manuscript, the authors utilized generative AI tools to enhance clarity and readability. All generated content was carefully reviewed, revised, and validated by the authors, who assume full responsibility for the accuracy and integrity of the final publication.

REFERENCES

[1] A. K. Maurya, C. Pandey, and R. Chhibber, "Dissimilar welding of duplex stainless steel with Ni alloys: A review," *International Journal of Pressure Vessels and Piping*, vol. 192, Aug. 2021, Art. no. 104439, https://doi.org/10.1016/j.ijpvp.2021.104439.

[2] M. Tümer, T. Mert, and T. Karahan, "Investigation of microstructure, mechanical, and corrosion behavior of nickel-based alloy 625/duplex stainless steel UNS S32205 dissimilar weldments using ERNiCrMo-3 filler metal," *Welding in the World*, vol. 65, no. 2, pp. 171–182, Feb. 2021, https://doi.org/10.1007/s40194-020-01011-0.

[3] L. Sharma and K. Sharma, "Dissimilar welding of super duplex stainless steel (SDSS) and pipeline steel – A brief overview," *Materials Today: Proceedings*, Dec. 2022, https://doi.org/10.1016/j.matpr.2022.12.057.

[4] K. Devendranath Ramkumar *et al.*, "Metallurgical and mechanical characterization of dissimilar welds of austenitic stainless steel and super-duplex stainless steel – A comparative study," *Journal of Manufacturing Processes*, vol. 19, pp. 212–232, Aug. 2015, https://doi.org/10.1016/j.jmapro.2015.04.005.

[5] L. Yang and N. Zhang, "Study on the Weldability of S32205 Steel under Different Welding Processes," *Advanced Materials Research*, vol. 239–242, pp. 793–796, 2011, https://doi.org/10.4028/www.scientific.net/AMR.239-242.793.

[6] L. Li *et al.*, "Comparative analysis of GTAW+SMAW and GTAW welded joints of duplex stainless steel 2205 pipe," *International Journal of Pressure Vessels and Piping*, vol. 199, Oct. 2022, Art. no. 104748, https://doi.org/10.1016/j.ijpvp.2022.104748.

[7] X. Hong, B. Huang, T. Li, P. Chen, J. Zheng, and Y. Zhu, "Effects of Welding Speed and Welding Current on the Residual Stress and Deformation of SAF 2507/316L Dissimilar Plasma Arc Welding," *Journal of Materials Engineering and Performance*, vol. 33, no. 24, pp. 13745–13763, Dec. 2024, https://doi.org/10.1007/s11665-023-08969-0.

[8] F. Badkoobeh, H. Mostaan, F. Nematzadeh, and M. Roshanai, "Nd: YAG laser beam welding of UNS N07718 superalloy and UNS S32304 duplex stainless steel: Phase transformations and mechanical properties of dissimilar joints," *Optics & Laser Technology*, vol. 170, Mar. 2024, Art. no. 110254, https://doi.org/10.1016/j.optlastec.2023.110254.

[9] M. Puchianu, H. F. Daşcău, and G. Solomon, "Studies Regarding FCAW Welding of Dissimilar Joints between Duplex Stainless Steel and Naval Carbon Steel," *Defect and Diffusion Forum*, vol. 416, pp. 43–54, 2022, https://doi.org/10.4028/p-i26fn3.

[10] G. Madhusudhan Reddy, T. Mohandas, A. Sambasiva Rao, and V. V. Satyanarayana, "Influence of Welding Processes on Microstructure and Mechanical Properties of Dissimilar Austenitic-Ferritic Stainless Steel Welds," *Materials and Manufacturing Processes*, vol. 20, no. 2, pp. 147–173, Mar. 2005, https://doi.org/10.1081/AMP-200041844.

[11] R. Kumar *et al.*, "Numerical and experimental investigation on distribution of residual stress and the influence of heat treatment in multi-pass dissimilar welded rotor joint of alloy 617/10Cr steel," *International Journal of Pressure Vessels and Piping*, vol. 199, Oct. 2022, Art. no. 104715, https://doi.org/10.1016/j.ijpvp.2022.104715.

[12] N. Kumar, P. Kumar, and C. Pandey, "Comparative study on the SMAW dissimilar welding of IN718 and ASS304L using ENiCrCoMo-1 and ENiCrFe-3 electrodes," *Materials Chemistry and Physics*, vol. 343, Oct. 2025, Art. no. 131080, https://doi.org/10.1016/j.matchemphys.2025.131080.

[13] A. Kumar and C. Pandey, "Structural integrity assessment of Inconel 617/P92 steel dissimilar welds for different groove geometry," *Scientific Reports*, vol. 13, no. 1, May 2023, Art. no. 8061, https://doi.org/10.1038/s41598-023-35136-1.

[14] A. K. Maurya, R. Chhibber, and C. Pandey, "Studies on residual stresses and structural integrity of the dissimilar gas tungsten arc welded joint of sDSS 2507/Inconel 625 for marine application," *Journal of Materials Science*, vol. 58, no. 20, pp. 8597–8634, May 2023, https://doi.org/10.1007/s10853-023-08562-9.

[15] A. Vinoth Jebaraj, T. Sampath Kumar, and M. Manikandan, "Investigation of Structure Property Relationship of the Dissimilar Weld Between Austenitic Stainless Steel 316L and Duplex Stainless Steel 2205," *Transactions of the Indian Institute of Metals*, vol. 71, no. 10, pp. 2593–2604, Oct. 2018, https://doi.org/10.1007/s12666-018-1392-y.

[16] N. Kumar, P. Kumar, and C. Pandey, "Impact of Buttering on Microstructure and Mechanical Behavior of IN718-ASS304L Dissimilar Joint," *Metallurgical and Materials Transactions A*, vol. 56, no. 8, pp. 3366–3390, Aug. 2025, https://doi.org/10.1007/s11661-025-07843-z.

[17] B. Yelamasetti, V. R. G., and T. Kadam, "Effect of filler wires on mechanical properties of super-duplex stainless steel UNS S32750 and austenitic stainless steel 304 dissimilar joints welded with PCGTAW technique.," *Songklanakarin Journal of Science & Technology*, vol. 44, no. 1, Jan. 2022 Art. no. 149.

[18] A. Taheri, B. Beidokhti, B. Shayegh Boroujeny, and A. Valizadeh, "Characterizations of dissimilar S32205/316L welds using austenitic, super-austenitic and super-duplex filler metals," *International Journal of Minerals, Metallurgy and Materials*, vol. 27, no. 1, pp. 119–127, Jan. 2020, https://doi.org/10.1007/s1261"3-019-1925-3.

[19] A. K. Maurya, A. Bhattacharyya, R. Chhibber, and C. Pandey, Structural integrity and corrosion behavior assessment of the dissimilar gas tungsten arc welded joint of sDSS 2507/ IN625 superalloy," *Materials Chemistry and Physics*, vol. 318, May 2024, Art. no. 129322, https://doi.org/10.1016/j.matchemphys.2024.129322.

[20] Syafrizal, A. Akhyar, M. Iqbal, and Syukran, "Selection of Optimal Filler Metal for Dissimilar Welding of SA335 Gr. P11 and Incoloy 800 in Primary Reformer Tube Catalyst Repairs: A Mechanical Property Analysis," *Engineering, Technology & Applied Science Research*, vol. 15, no. 6, pp. 29887–29893, Dec. 2025, https://doi.org/10.48084/etasr.14269.

[21] "Welding Handbook Quick View || Products || KOBELCO - KOBE STEEL, LTD. -." https://ftp.kobelco-welding.jp/handbook/products/view/118/.

[22] E. Taban, E. Kaluc, and T. S. Aykan, "Effect of the Purging Gas on Properties of 304H GTA Welds," vol. 93, pp. 124–130, Apr. 2014.

[23] *ASME B31.3 Process Piping*. USA: American Society of Mechanical Engineers, 2020.

[24] ASME Boiler and Pressure Vessel Committee on Nondestructive Examination. USA: American Society of Mechanical Engineers, 2019.

[25] ASTM E23-16b Standard Test Methods for Notched Bar Impact Testing of Metallic Materials. USA: ASTM International, 2018.

[26] C. Pandey, M. M. Mahapatra, P. Kumar, F. Daniel, and B. Adhithan, "Softening mechanism of P91 steel weldments using heat treatments," *Archives of Civil and Mechanical Engineering*, vol. 19, no. 2, pp. 297–310, June 2019, https://doi.org/10.1016/j.acme.2018.10.005.

[27] W. N. Khan and R. Chhibber, "Effect of filler metal on solidification, microstructure and mechanical properties of dissimilar super duplex/pipeline steel GTA weld," *Materials Science and Engineering: A*, vol. 803, Jan. 2021, Art. no. 140476, https://doi.org/10.1016/j.msea.2020.140476.

[28] G. Sharma and B. S. Chauhan, "Impact of filler metal on microstructural and mechanical performance of ASS304L/DSS2205 steel dissimilar GTA weld," *Welding International*, pp. 1–11, Dec. 2025, https://doi.org/10.1080/09507116.2025.2594668.

[29] ASTM 923 -03 Standard Test Methods for Detecting Detrimental Intermetallic Phase in Duplex Austenitic/Ferritic Stainless Steels. USA: ASTM International, 2023.

[30] B31.3-2012 Process Piping, ASME Code for Pressure Piping. USA: American Society of Mechanical Engineers, 2012.

[31] J. Verma, R. V. Taiwade, and R. Sonkusare, "Effects of austenitic and duplex electrodes on microstructure, mechanical properties, pitting, and galvanic corrosion resistance of ferritic and dual-phase stainless steel dissimilar joints," *Journal of Materials Research*, vol. 32, no. 16, pp. 3066–3077, Aug. 2017, https://doi.org/10.1557/jmr.2017.269.